Measurement of higher harmonic flow coefficients of identified hadrons in Pb-Pb collisions at $\sqrt{s_{\rm NN}} = 2.76$ TeV

Naghmeh Mohammadi for the ALICE collaboration

Nikhef, Science Park 105, 1098 XG, Amsterdam, The Netherlands

E-mail: naghmehmohammadi@cern.ch

Abstract. The latest ALICE results on the centrality and transverse momentum dependence of v_2, v_3, v_4 and v_5 for $\pi^{\pm}$, $\rm K^{\pm}$ and $\rm p(\bar{p})$ in Pb–Pb collisions at $\sqrt{s_{\rm NN}} = 2.76$ TeV are presented. The flow coefficients exhibit a clear mass ordering for $p_{\rm T} < 2.5$ GeV/c for all harmonics. For transverse momentum values larger than about 3 GeV/c, mesons exhibit distinctively lower flow values compared to baryons, suggesting that coalescence might be the relevant particle production mechanism in this region. The experimental data for $p_{\rm T} < 2.5$ GeV/c are described fairly well by the hydrodynamical model iEBE-VISHNU, which models the hydrodynamical expansion of the fireball using a value of $\eta/s = 0.08$, coupled to a hadronic cascade model (UrQMD). Finally, A Multi-Phase Transition Model (AMPT) highlights the significant contribution of the hadronic rescattering phase and of coalescence as the dominant particle production mechanism to the mass ordering at low $p_{\rm T}$ and the baryon-meson grouping at intermediate $p_{\rm T}$, respectively.

Keywords: QGP, ALICE, azimuthal anisotropy, shear viscosity, iEBE-VISHNU, UrQMD, AMPT

1. Introduction

The aim of the heavy ion collision experiments is to study the Quark Gluon Plasma (QGP) [1] and constrain its transport properties such as the ratio of shear viscosity to entropy density (η/s) and equation of state. One of the observables sensitive to the properties of the QGP is anisotropic flow which characterises the momentum anisotropy of the final state particles. This momentum anisotropy rises from the spatial anisotropy of the overlapping collision region through interactions between partons and at later stages between the produced particles. The momentum anistropy can be expressed in terms of a Fourier expansion of the particle distribution $dN/d(\varphi - \Psi_n)$ in azimuthal angle φ with respect to the $n^{\rm th}$-order symmetry plane angle Ψ_n [2], according to:

$$dN/d(\varphi - \Psi_n) \approx 1 + \sum_n 2v_n \cos[n(\varphi - \Psi_n)]. \quad (1)$$

In this equation, v_n is the $n^{\rm th}$-order flow coefficient and can be calculated according to $v_n = \langle \cos[n(\varphi - \Psi_n)] \rangle$, where the brackets denote an average over all events and particles.

In this article, we report the $p_{\rm T}$-differential elliptic (v_2), triangular (v_3), quadrangular (v_4) and pentagonal (v_5) flow for $\pi^{\pm}$, $\rm K^{\pm}$ and $\rm p(\bar{p})$ in two different centrality intervals of Pb–Pb collisions at $\sqrt{s_{\rm NN}} = 2.76$ TeV measured with the ALICE detector.

2. Analysis details

The analysis is performed on both Pb–Pb and pp collisions at $\sqrt{s_{\rm NN}} = 2.76$ TeV recorded by ALICE during 2011 at the LHC [3]. For Pb–Pb collisions the minimum bias events are triggered by the coincidence between the signals from both sides of the V0 detectors. In addition, an online selection based on the V0 detectors are used in Pb–Pb collisions to increase the number of central (i.e. 0–10% centrality interval) and semi-central (i.e. 10–50%) collisions. For minimum bias pp collisions at least one hit is required in the SPD (the innermost layer of the Inner Tracking System) or V0 detectors.

The reconstructed primary vertex position along the z axis (z_{vtx}) for all analysed events are required to be within 10 cm from the nominal interaction point. In addition, events with multiple reconstructed primary vertices are rejected which leads to a negligible amount of pile-up events for all systems [4]. After applying all the selection critera, a filtered data sample with 25×10^6 events are analysed for Pb–Pb and 20×10^6 for pp collisions to produce the results presented in this article. The two centrality intervals presented in this article are 0–1% (i.e. smallest impact parameter) and 20–30% (i.e. larger impact parameter) centrality intervals in Pb–Pb collisions.

The track reconstruction is performed using the information from both the Time Projection Chamber (TPC) and the Inner Tracking System (ITS). The charged particle momenta is measured using both ITS and TPC with an azimuthal coverage of $|\eta| < 0.9$. The particle identification (PID) for pions ($\pi^{\pm}$), kaons ($K^{\pm}$) and protons ($p + \bar{p}$) used in this analysis is based on a procedure reported in [5] which combines the signals from the TPC and Time Of Flight (TOF) detectors. In this analysis, different particle species are identified by requiring a minimum identification probability of 90%. More details on the PID procedure followed can be found in [6].

The flow coefficients are measured with the Scalar Product method [7]. The identified particle of interest (POI), i.e. pions ($\pi^{\pm}$), kaons ($K^{\pm}$) and protons ($p + \bar{p}$), and the charged reference particles (RP) are selected from two non-overlapping subevents within the acceptance of the TPC detector ($-0.8 < \eta < 0$ and $0 < \eta < 0.8$). Correlations not related to the common symmetry plane, denoted as $\delta_n^{AA,pp}$, are estimated using minimum bias pp collisions and are subtracted from the measured flow coefficients in Pb-Pb collisions denoted as v_n^{AA} with a procedure described in [6]. In this article, the reported values, v_n^{sub}, are extracted according to $v_n^{sub} = v_n^{AA} - \delta_n^{AA,pp}$.

3. Results and discussions

Figure 1 presents the $p_{\rm T}$-differential v_2^{sub}, v_3^{sub}, v_4^{sub} and v_5^{sub} for charged pions, kaons and (anti-)protons for the 0–1% (upper row - ultra-central collisions) and 20–30% (bottom row - mid-central collisions) centrality intervals in Pb–Pb collisions at $\sqrt{s_{\rm NN}} = 2.76$ TeV. In the ultra-central collisions, where the evolution of the system is mainly dominated by initial state fluctuations, one observes significant non-zero values for all harmonics and particle species. In addition, the magnitude of higher flow harmonics are comparable to that of elliptic flow. However, in mid-central collisions, the magnitude of elliptic flow is significantly larger than in ultra-central collisions and rises to become the dominant flow harmonic. The magnitude of higher harmonics also has increased with respect to the ultra-central collisions but this increase is not as significant as the one of elliptic flow. These observations confirm that elliptic flow is mainly driven by the anisotropy of the collision geometry. However, higher flow harmonics are less dependent on the geometry and more driven by the initial state fluctuations. This can be quantified by taking the ratio of v_n^{sub} in ultra- to mid-central collisions. For elliptic flow and for all particle species, this ratio is at most 25%, whereas for v_3^{sub} the ratio is >60%.

Furthermore, a clear mass ordering can be seen in all harmonics and centrality intervals in the low $p_{\rm T}$ region (i.e. $p_{\rm T} \leq 2.5$ GeV/c) which rises from the interplay between the anisotropic flow harmonics and radial flow. Radial flow creates a depletion in the low $p_{\rm T}$ region of the particle spectrum which is more pronounced in- than out-of-plane with increasing particle mass. This

leads to a lower v_n^{sub} value for heavier particles. In addition, $v_{n(=2,3,4)}^{sub}$ show a clear baryon-meson grouping in the intermediate $p_{\rm T}$ region in which v_n^{sub} of baryons is larger than the values for mesons.

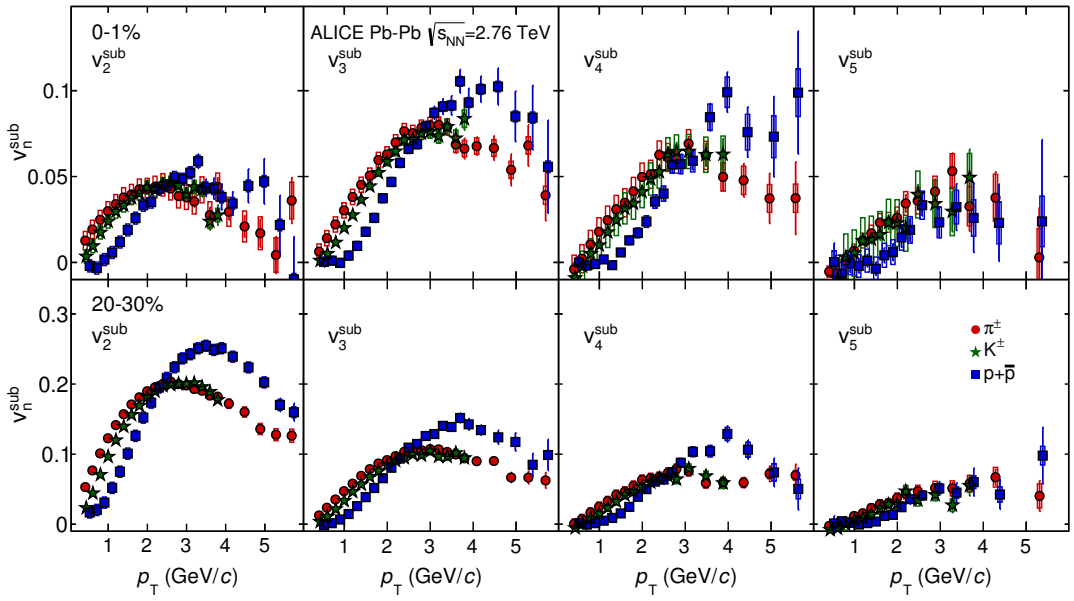

Figure 1. The $p_{\rm T}$-differential v_2^{sub} (first column), v_3^{sub} (second column), v_4^{sub} (third column), and v_5^{sub} (fourth column), for different particle species for the 0–1% (upper row) and the 20–30% (lower row) centrality intervals of Pb–Pb collisions at $\sqrt{s_{\rm NN}} = 2.76$ TeV [6].

A comparison is performed between v_n^{sub} $(n = 2-4)$ and recent v_n hydrodynamical calculations from [8]. These calculations are based on iEBE-VISHNU, an event-by-event version of the VISHNU hybrid model coupling 2+1 dimensional viscous hydrodynamics (VISH2+1) to a hadronic cascade model (UrQMD). In this model, the ratio of shear viscosity to entropy density is fixed to $\eta/s = 0.08$. The model describes the v_2^{sub} measurements for all particles and centrality intervals within 10-15%. The model predictions show a better agreement (within 5% deviations) with the measured v_3^{sub} and v_4^{sub}.

In this analysis, three different versions of A Multi-Phase Transport Model (AMPT) are investigated. AMPT can run over two configurations, namely the default and the string melting. In both configurations, the final state hadronic rescattering phase is implemented which also includes resonance decays. In the string melting configuration, final state hadrons are formed via a quark coalescence mechanism. The third version is based also on the string melting configuration with the hadronic rescattering phase switched off. More details on the AMPT configurations used in this analysis can be found in [6].

Figure 2 presents the $p_{\rm T}$-differential v_3 for charged pions, kaons and (anti-)protons for the 20-30% centrality interval measured with the Scalar Product method. Each panel presents the results of one of the three AMPT versions introduced above. The string melting version (left) predicts a clear mass ordering at low $p_{\rm T}$ as well as a clear baryon-meson grouping at the intermediate $p_{\rm T}$. The string melting version without hadronic rescattering (middle), however, can only reproduce the baryon-meson grouping and the default version (right) is only able to reproduce the mass ordering at low values of $p_{\rm T}$. These observations emphasize the effect of hadronic rescattering in the development of the mass ordering at the low $p_{\rm T}$ region and the

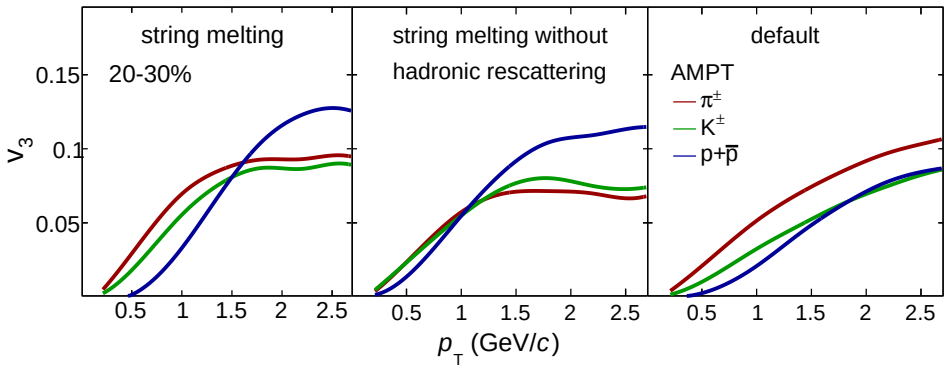

Figure 2. The p_{T}-differential v_3 in 20-30% Pb–Pb collisions at $\sqrt{s_{\mathrm{NN}}} = 2.76$ TeV obtained using the string melting, with (left) and without (middle) hadronic rescattering, and the default (right) versions.

coalescence for the baryon-meson grouping at the intermediate p_{T} region.

4. Summary

In this article, the non-flow subtracted flow harmonics, v_2^{sub}, v_2^{sub}, v_2^{sub} and v_2^{sub} are reported as a function of transverse momentum for charged pions, kaons and (anti-)protons at 0-1% and 20-30% centrality intervals in Pb–Pb collisions at $\sqrt{s_{\mathrm{NN}}} = 2.76$ TeV. The v_n measurements are performed using the Scalar Product method where identified hadrons and reference charged particles are selected from two non-overlapping subevents. The non-flow contribution, i.e. correlations unrelated to the common symmetry plane, is estimated using pp collisions and then subtracted from the v_n measurements.

All flow harmonics exhibit an increase in magnitude in more peripheral collisions. This increase is more significant for elliptic flow compared to higher harmonics which indicates that v_2 is more dependent on the anisotropy of the collision geometry. On the other hand, higher harmonics are more driven by the initial state fluctuations. A distinct mass ordering is seen in low p_{T} region which is attributed to the interplay between radial flow and anisotropic flow harmonics. In addition, AMPT measurements highlight the importance of the final state hadronic rescattering phase in the development of the mass ordering of v_n in this p_{T} region. In the intermediate p_{T} values, a baryon-meson grouping is seen where baryons show a higher magnitude compared to mesons. This is observed also in the AMPT string melting version which demonstrates the effect of quark coalecence in this p_{T} region.

References

[1] S. A. Bass, M. Gyulassy, H. Stoecker and W. Greiner, J. Phys. G **25** (1999) R1 [hep-ph/9810281].
[2] S. Voloshin and Y. Zhang, Z. Phys. C **70** 665 (1996) [hep-ph/9407282].
[3] K. Aamodt *et al.* [ALICE Collaboration], JINST **3**, S08002 (2008).
[4] B. B. Abelev *et al.* [ALICE Collaboration], Int. J. Mod. Phys. A **29**, 1430044 (2014) [arXiv:1402.4476 [nucl-ex]].
[5] J. Adam *et al.* [ALICE Collaboration], Eur. Phys. J. Plus **131**, no. 5, 168 (2016) [arXiv:1602.01392 [physics.data-an]].
[6] J. Adam *et al.* [ALICE Collaboration], arXiv:1606.06057 [nucl-ex].
[7] S.A. Voloshin, A.M. Poskanzer, R. Snellings, in: Landolt-Boernstein, Relativistic Heavy Ion Physics, vol. 1/23, Springer-Verlag, pp. 554, 2010.
[8] H. j. Xu, Z. Li and H. Song, Phys. Rev. C **93**, no. 6, 064905 (2016) [arXiv:1602.02029 [nucl-th]].